IMAGING AMYLOID PRECURSOR PROTEIN *IN VIVO* – AN AXONAL TRANSPORT ASSAY

Tomás L. Falzone[1] and Gorazd B. Stokin[2*]

[1]Instituto de Biología Celular y Neurociencias, CONICET, Facultad de Medicina, UBA. Paraguay 2155, 3[er] Piso, Buenos Aires, Argentina 1121, tfalzone@fmed.uba.ar;

[2]University Psychiatric Hospital, Studenec 48 and Division of Neurology, University Medical Center, Zaloška 2, Ljubljana, Slovenia, gbstokin@alumni.ucsd.edu

*Corresponding author

Running head: Axonal transport assay

Summary

Fusion of fluorescent probes to axonally transported proteins represents an established approach that enables live imaging of axonal transport. In this approach, *in vivo* examination of fluorescent particle dynamics provides information about the length, directionality and the velocity by which axonally transported proteins travel along axons. Analysis of these parameters provides information about the distribution of axonal proteins and their dynamics in and between different subcellular compartments. Establishing the movement behavior of amyloid precursor protein within axons indicated that live imaging approaches offer the opportunity to significantly enhance our understanding of the biology as well as pathology of axonal transport. This chapter provides a fluorescence-based procedure for measuring axonal transport of APP in cultured newborn mouse hippocampal neurons.

Key words: Fluorescent probes, Amyloid precursor protein, Axonal transport, Primary hippocampal cell culture, *In vivo* fluorescent imaging

1. Introduction

Axonal transport is a complex system that guarantees the delivery of proteins and organelles to synapses, axonal compartments and cell bodies in a timely manner. This transport system, which supplies high synaptic protein turnover with the appropriate cell-derived commands and delivers environmental signals from different presynaptic environments to cell bodies, relies on molecular motors moving cargoes along microtubule tracks at the expense of ATP hydrolysis. The force generating molecular motors transport cargoes either towards the synapses or towards cell bodies by means of anterograde and retrograde axonal transport, respectively (***1***).

Amyloid precursor protein (APP) is a type II integral membrane protein (***2***). In neurons, APP containing vesicles undergo constitutive bidirectional axonal transport. Several observations link APP to the pathogenesis of Alzheimer's disease (AD). In brief, aberrant *App* genotypes segregate with AD phenotype (***3***) and aberrant accumulation of proteolytic fragments of APP in the form of amyloid peptides and plaques are considered a neuropathological hallmark of AD brains (***4***). Intriguingly, aberrant accumulation of APP and its proteolytic fragments has been long described within axons of AD brains (***5***) as well as in several other diseases ranging from traumatic brain injury to multiple sclerosis. The early pathological presence of APP in the axons points to a role of APP beyond AD, suggesting that APP may represent a *bona fide* surrogate marker of axonal injury **(*6,7*)**.

Early work on axonal APP focused largely on immunochemical studies. These approaches indisputably localized APP within axons and uncovered its aberrant accumulation in disease **(*8*)**. Axonal transport of APP was first suggested in a sciatic nerve ligation study, which showed APP synthesized in the dorsal root ganglia accumulating proximally to the ligation site within axons **(*9*)**. It was after the

development of fluorescent approaches, however, when bidirectional movement of APP was first visualized, together with the assessment of its dynamic behavior within axons **(*10, 11*)**. Although the function of axonal APP movement behavior and the mechanisms regulating axonal transport of APP remain largely unknown, these approaches indisputably revolutionized our understanding of APP biology and allowed the identification of APP axonal transport impairments in animal models of AD, which added a new twist to the current pathogenesis of AD **(*12-15*)**. In conclusion, novel fluorescent approaches to studying axonal transport can be applied to any axonally transported transmembrane or soluble protein. The tracking and surveillance of these proteins have only started producing a wealth of new data that will significantly further our understanding of the axonal milieu **(*16,17*)**. The present chapter describes a detailed protocol in which the above approach is applied to the axonal tracking of APP in cultured mouse hippocampal neurons.

2. Materials

2.1. Primary Hippocampal Neuron Cultures

1. Cold Hank's balanced salt solution (HBSS, Gibco). Store at 4°C (*see* **Notes 1-4**).
2. Hank's buffer: To 500 mL HBSS, add 0.4 g of D-glucose (Sigma-Aldrich), 0.834 g of 4-(2-hydroxyethyl)-1-piperazineethanesulfonic acid (HEPES, Sigma-Aldrich), 5 ml of 100X penicillin-streptomycin (Invitrogen) and filter sterilize using 0.22 µm diameter filter cartridge. Store at 4°C.
3. Disaggregation buffer: add to phosphate buffered saline (PBS, Gibco) 1.5 mM DL-cysteine HCL (Sigma-Aldrich), 0.025% bovine serum albumin (BSA, Sigma-Aldrich) and 35 mM D-glucose (Sigma-Aldrich). Store at -20°C.

4. Papain solution: add 45 Units of lyophilized papain (Worthington) and 0.05% DNase I (Boehringer Mannheim) to disaggregation buffer. Once papain is dissolved filter-sterilize by passing through a 0.22 µm diameter filter cartridge.
5. Complete Dulbecco's Modified Eagle's Medium (DMEM, Gibco): supplement DMEM with 10% fetal bovine serum (FBS, Gibco) and 500 µM L-glutamine (Sigma-Aldrich). Store at 4°C.
6. Complete Neurobasal medium: enrich neurobasal medium (Gibco) with 1:50 (v/v) of 50X serum-free supplement B27 (Invitrogen) and 500 µM L-glutamine (Sigma-Aldrich). Store at 4°C.
7. Boric acid buffer: To 400 mL of water add 1.24 g of boric acid (Sigma-Aldrich) and 1.9 g of borax (Sigma-Aldrich), then filter sterilize the solution. Store at 4°C.
8. Poly-D-lysine-coated coverslips: wash round coverslips (Fisher Scientific) 3 times using 100% acetone with gentle agitation, then 3 times with 100% ethanol and finally 3 times with sterile water. When dried, coverslips are incubated with 100 µg of poly-D-lysine (MW 30,000-70,000) per mL of boric acid buffer for several hours at room temperature, then washed thoroughly with sterile water and placed in a 24-well dish (Falcon, BDbiosciences) for cell plating.
9. Stereo dissecting scope (SMZ660, Nikon)
10. Fine forceps and scissors (Roboz)

2.2. Transfection

1. Pcdna3 CMV-APP-YFP vector expressing a protein fusion between APP695 (APP) and yellow fluorescent protein (YFP) at the C-terminus of APP (*see* **Note 5**) **(*10*)**
2. Lipofectamine 2000 (Invitrogen). Store at 4°C.
3. 10 days-old primary hippocampal cell culture

2.3. Axonal Transport Imaging

1. Inverted epi-fluorescent microscope (TE-2000U, Nikon)
2. Heat and CO_2 controlled chamber (Harvard Apparatus, Holliston, MA)
3. Photometrics CoolSNAP$_{HQ}$-cooled CCD camera (Roper Scientific, Ottobrunn, Germany)
4. Glass bottom plates (MatTek, Ashland, MA)
5. MetaMorph 6.0 (Universal Imaging Corporation, Marlow, UK)

3. Methods

3.1. Harvesting Cells from Hippocampi

1. Primary hippocampal cell cultures are harvested from post-natal day 1 mice (*see* **Note 6**). Using fine forceps under a dissecting scope cut the skin above calvarium by a midline anteroposterior incision. Separate from the underlying bones of the calvarium both skin flaps generated by the incision. Incise the cranial bones in the top midline portion and chip away to expose the brain.
2. Detach the brain from the cranial nerves, remove from the skull and cut in half. Use a small spoon to remove the hippocampi from the brain and meninges, and place into cold HBSS (*see* **Note 7**).
3. Under a tissue culture hood, wash the excised hippocampi with 10 mL of

HBSS at 4°C and then digest in 0.22 µ-filtered papain disaggregation buffer for 20 minutes with moderate shaking at 37°C.

4. After digestion, wash hippocampi twice with 10 mL of complete DMEM (*see* **Note 8)**, triturate 12 times with a 1 mL micro-pipette in 2 mL of complete DMEM and plate on top of poly-D-lysine-coated coverslips at 60,000 cells per well in a 24-well dish (*see* **Note 9**).
5. After allowing 2 hours for neurons to attach, replace the complete DMEM with 500 µL of complete Neurobasal medium. Maintain cell cultures at 37ºC in 5% CO_2 incubator.

3.2. Transfection

Ten-to-fourteen-day old primary hippocampal cell cultures are transfected with pcdna3 CMV-APP-YFP expression vector using Lipofectamine 2000.

1. For each well, dilute 0.8 µg of endotoxin-free purified DNA in 50 µL of plain Neurobasal medium and gently mix. Similarly, gently mix and dilute 2 µL of Lipofectamine 2000 in 50 µL of plain Neurobasal medium and then incubate for 5 minutes.
2. After incubation, combine the diluted DNA with diluted Lipofectamine 2000 to a total volume of 100 µL, mixed gently and incubate for 20 minutes.
3. Remove 300 µL of complete Neurobasal medium from each well and add 100 µL of DNA-Lipofectamine complexes to each well containing primary hippocampal cells (*see* **Note 10**). Mix gently by rocking the plate back and forth.
4. Incubate cells at 37ºC in a 5% CO2 incubator, and replace medium to complete Neurobasal medium 2-4 hours later (*see* **Note 11**).

3.3. *In vivo* Imaging

1. *In vivo* transport of APP-YFP vesicles is imaged 16 hours after transfection using a heated stage at 37ºC and in a 5% CO_2 chamber using an inverted epifluorescent microscope connected to a Photometrics CoolSNAP$_{HQ}$-cooled CCD camera and driven by MetaMorph 6.0. (*see* **Note 12**)
2. Remove transfected cells from multiwell plates by lifting the coverslip with forceps and flipping it over a glass bottom plate containing complete Neurobasal medium equilibrated in a 5% CO_2 incubator (*see* **Note 13**).
3. Identify fluorescent (transfected) cell bodies using an oil immersion super apochromatic 100X lens. Follow axonal projections at least two fields away from the cell body view. Anterograde and retrograde axonal transport is determined depending on the orientation of cell bodies and projection tips.
4. Register axonal dynamics of fluorescent APP-YFP vesicles in 15-second stacks format (tiff) and capture at a speed of 10 frames per second at 100X magnification and 2x2 binning for continuous registration (*see* **Note 14**, **Fig. 1**). Kymographs are generated from stacks and analyzed using MetaMorph or converted to QuickTime or AVI movie format for presentations. Calibration of movie pixel magnification and number of frames per second should be established prior movie registration and used across experiments.

3.4. Kymograph Generation and Analysis

1. Open movie stack in a working station computer using MetaMorph (*see* **Note 15**). Draw a line of 5 pixel width from cell body to axon tip to define the

precise location of the measurements and to track the length of the axon in captured movies.

2. Using the kymograph function in MetaMorph generate a montage image from the plotted line in which distance and time are represented by the X and Y axes, respectively (**Fig. 2a**).
3. Using MetaMorph, in each kymograph plot lines following all visible straight and descending fluorescent particles generated by APP vesicle dynamics along time (**Fig. 2b**). Transfer measurements extracted from lines such as angle, X and Y, start and end points obtained from pixel identification to an excel file and convert to microns by time for analysis (**Fig. 3a**). APP-YFP vesicle movement is approximated from kymograph as a percentage of clearly defined stationary, anterogradely- or retrogradely-moving APP-YFP out of defined particles, which started and ended movement within the time and distance captured in the kymograph. Average speed, distance and directionality of axonal transport are calculated in excel files for further statistical analysis (**Fig. 3b**).
4. In line with scientific rigor, all kymographs are coded before the beginning of each experiment and scored blind to the identity of the sample. Only upon completion of particle plotting and of all data collection the samples are uncoded to allow analysis.

4. Notes

1. Prepare all solutions using ultrapure water by purifying deionized water to attain a sensitivity of 18 MΩ cm at 25°C.

2. Prepare, store and manipulate all reagents at room temperature unless indicated otherwise.
3. Follow regulations strictly for disposal of waste materials.
4. Hank's buffered salt solution is fairly complicated to make, which is why most people buy it.
5. Any APP cDNA, or other axonally transported protein cDNA, fused to a fluorescent probe can be used for the *in vivo* imaging of protein movement within axons. Alternatively, or simultaneously, fluorescent dies may be used for labeling proteins or organelles. In example, mitochondria can be dynamically visualized using Mitotracker (Invitrogen).
6. Unless otherwise stated all steps of the described method are performed at room temperature and pressure.
7. Hippocampal spoon (Fine Science Tools) can be used to facilitate detachment of hippocampi from cornu Ammonis.
8. Complete DMEM used for washing allows FBS to inactivate papain activity.
9. Pipette trituration is a key step. Do it too much and you'll kill the cells, do it too little and you'll have many clumps.
10. Little drops can be delivered at different points of the round cover slips to facilitate distribution. Make sure the medium covers the entire well surface.
11. The same medium removed before starting transfection can be used to replace lipofectamine transfection medium. This procedure helps cells recover after transfection due to factors and proteins released by cells during their development.
12. Continued registration can be done with different camera software devises in TIFF format and then opened in a different computer station for analysis.

13. High magnifications (100X) require a short working distance from specimen to lens. The sandwich made by flipping the cover slips inside the glass bottom plate (1mm) allows the cells to be in the lens working distance for imaging and movie registration.
14. Cooled CCD camera allows fast continuous registration at low sensitivity reaching the speed of 10 frames per second at a time resolution of 100 msecond per frames. 2x2 binning was set up to favor high speed acquisition by reducing the recorded information.
15. Kymograph can also be generated in imageJ software using "multiple kymograph" plug-in.

Acknowledgements

This work was supported by PICT-2008-0293 (ANPCyT)(T.L.F.), Alzheimer Association NIRG-10-172840 Grant (T.L.F.) and P3-0338 grant from the Slovenian Research Agency (G.B.S.).

References

1. Hirokawa N, and Noda Y (2008) Intracellular transport and kinesin superfamily proteins, KIFs: structure, function, and dynamics. *Physiol Rev 88*, 1089-1118
2. Kang J, Lemaire HG, Unterbeck A, Salbaum JM, Masters CL, Grzeschik KH, et al (1987) The precursor of Alzheimer's disease amyloid A4 protein resembles a cell-surface receptor. *Nature 325*, 733-736
3. Bertram L, Lill CM, and Tanzi R E (2010) The genetics of Alzheimer disease: back to the future. *Neuron 68*, 270-281
4. Goedert M, and Spillantini MG (2006) A century of Alzheimer's disease. *Science 314*, 777-781
5. Cras P, Kawai M, Lowery D, Gonzalez-DeWhitt P, Greenberg B, and Perry G (1991) Senile plaque neurites in Alzheimer disease accumulate amyloid precursor protein. *Proc Natl Acad Sci U S A 88*, 7552-7556
6. Stokin GB, and Goldstein LS (2006) Axonal transport and Alzheimer's disease. *Annu Rev Biochem 75*, 607-627
7. Stokin GB, and Goldstein LS (2006) Linking molecular motors to Alzheimer's disease. *J Physiol Paris 99*, 193-200
8. Joachim CL, Duffy LK, Morris JH, and Selkoe DJ (1988) Protein chemical and immunocytochemical studies of meningovascular beta-amyloid protein in Alzheimer's disease and normal aging. *Brain Res 474*, 100-111
9. Koo EH, Sisodia SS, Archer DR, Martin LJ, Weidemann A, Beyreuther K, et al (1990) Precursor of amyloid protein in Alzheimer disease undergoes fast anterograde axonal transport. *Proc Natl Acad Sci U S A 87*, 1561-1565

10. Kaether C, Skehel P, and Dotti CG (2000) Axonal membrane proteins are transported in distinct carriers: a two-color video microscopy study in cultured hippocampal neurons. *Mol Biol Cell 11*, 1213-1224

11. Goldsbury C, Thies E, Konzack S, and Mandelkow EM (2007) Quantification of amyloid precursor protein and tau for the study of axonal traffic pathways. *J Neurosci 27*, 3357-3363

12 Stokin GB, Lillo C, Falzone TL, Brusch RG, Rockenstein E, Mount SL, et al (2005) Axonopathy and transport deficits early in the pathogenesis of Alzheimer's disease. *Science 307*, 1282-1288

13. Stokin GB, Almenar-Queralt A, Gunawardena S, Rodrigues EM, Falzone T, Kim J, et al (2008) Amyloid precursor protein-induced axonopathies are independent of amyloid-beta peptides. *Hum Mol Genet 17*, 3474-3486

14. Falzone TL, Stokin GB, Lillo C, Rodrigues EM, Westerman EL, Williams DS, et al (2009) Axonal stress kinase activation and tau misbehavior induced by kinesin-1 transport defects. *J Neurosci 29*, 5758-5767

15. Araki Y, Kawano T, Taru H, Saito Y, Wada S, Miyamoto K, et al (2007) The novel cargo Alcadein induces vesicle association of kinesin-1 motor components and activates axonal transport. *EMBO J 26*, 1475-1486

16. Eva R, Dassie E, Caswell PT, Dick G, ffrench-Constant C, Norman JC, et al (2010) Rab11 and its effector Rab coupling protein contribute to the trafficking of beta 1 integrins during axon growth in adult dorsal root ganglion neurons and PC12 cells. *J Neurosci 30*, 11654-11669

17. Bilsland LG, Sahai E, Kelly G, Golding M, Greensmith L, and Schiavo G (2010) Deficits in axonal transport precede ALS symptoms in vivo. *Proc Natl Acad Sci U S A 107*, 20523-20528

Figure Legends

Figure 1: Axonal transport movie registered in primary hippocampal neurons transfected with APP-YFP using an inverted epi-fluorescent microscope. 100 msecond frame image montage of a movie registered in a transfected axon showing dynamics of APP-YFP vesicles. White arrows indicate stationary (1,4,7), anterograde (2,3) or retrograde (5,6) moving vesicles, respectively. Time correspond to frames extracted from a 30 second movie. Bar equals 10 µmeters.

Figure 2: Kymograph generated from movie showing APP-YFP axonal transport dynamics. a) Kymograph generated from movie in **Fig. 1** showing the distance displacement of anterograde, stationary, and retrograde APP-YFP vesicles along 30 seconds. **b)** Schematic representation of the above kymograph in which all APP-YFP vesicles were tracked and plotted. Straight, dashed, and dotted black lines correspond to anterograde (2,3), retrograde (5,6), and stationary (1,4,7) particles, respectively. Bar equals 10 µmeters.

Figure 3: Axonal transport measurements obtained from kymograph analysis. a) Excel file showing calculations extracted from lines plotted on Kymograph from **Fig. 2b**. Each line was separated by decreasing angle and corresponds to anterograde, stationary, and retrograde particles. Distance, time and speed are calculated from the kymograph. **b)** Results of average particle proportion (%), speed (µm/sec), and run length (µm) calculated from excel file. Black, gray, and white bars correspond to anterograde, stationary and retrograde transport, respectively.

Figure 1:

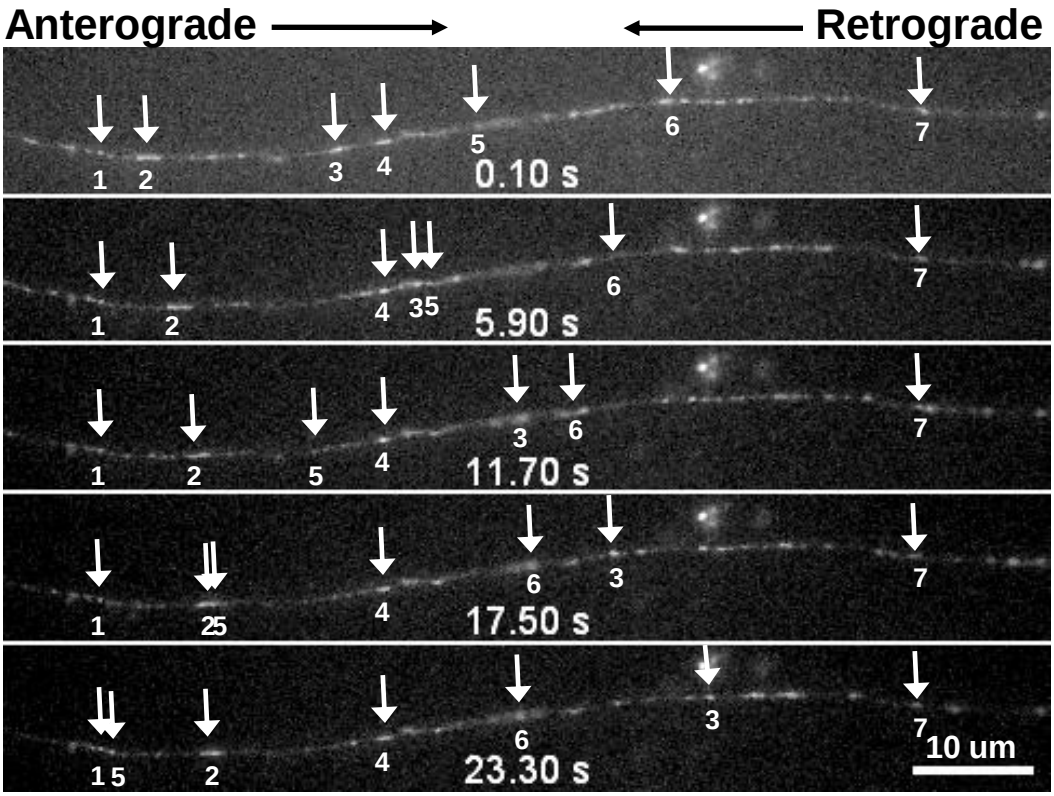
Anterograde
Retrograde
1
2
3
4
5
6
7
0.10 s
1
2
4
35
6
7
5.90 s
1
2
5
4
3
6
7
11.70 s
1
25
4
6
3
7
17.50 s
15
2
4
6
3
7
23.30 s
10 um

Figure 2:

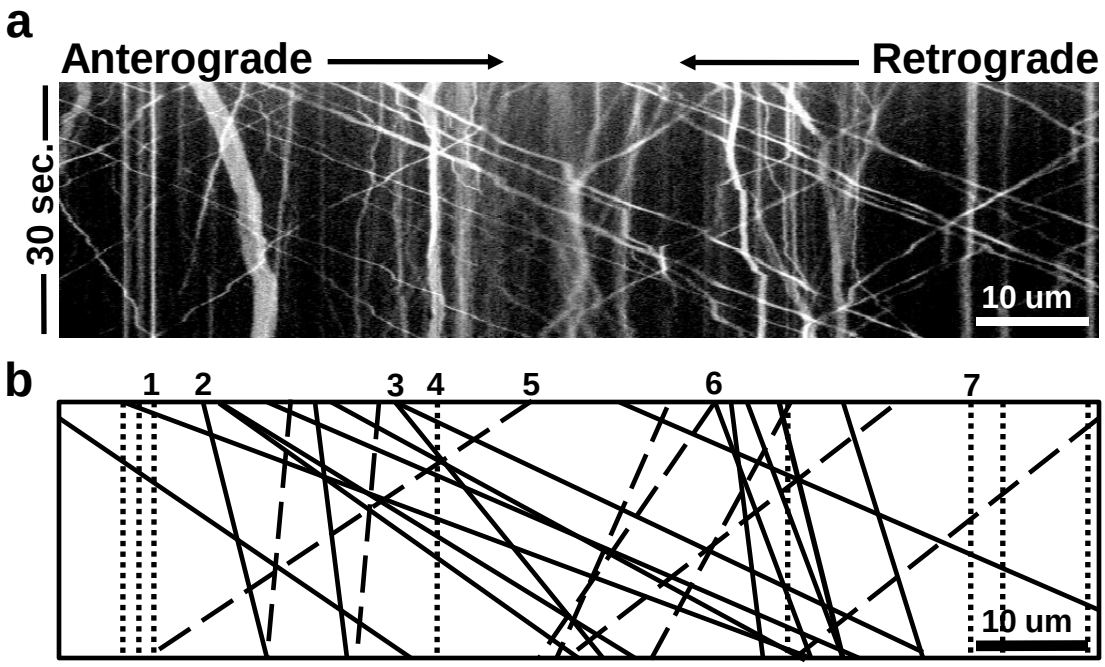

Figure 3:

a

	Features	Angle	Distance in pixels	Distance in um	Time (Sec)	Speed (distance/time)
	L5	110.0254	653	87.64566	29.75	2.946072605
	L11	113.0494	557	74.76054	29.75	2.512959328
	L21	113.2764	444	59.59368	23.875	2.496070366
	L14	115.5885	497	66.70734	29.75	2.242263529
	L12	121.1345	394	52.88268	29.75	1.777569076
Anterograde	L32	123.6502	332	44.56104	29.75	1.497850084
	L7	126.4692	322	43.21884	29.75	1.452734118
	L16	137.5114	218	29.25996	29.75	0.983528067
	L1	147.3438	141	18.92502	29.625	0.638819241
	L22	160.4841	84	11.27448	29.75	0.378974118
	L23	164.2774	67	8.99274	29.75	0.302276975
	L24	166.5316	57	7.65054	29.75	0.257161008
	L6	166.7595	56	7.51632	29.75	0.252649412
	L18	174.2417	24	3.22128	29.75	0.108278319
	L9	174.9364	21	2.81862	29.625	0.095143291
	L15	179.2778				
	L20	179.2778				
	L27	179.2778				
	L2	179.5165				
Stationary	L3	180				
	L4	180				
	L26	180.2407				
	L25	180.9629				
	L13	186.2606	26	3.48972	29.75	0.117301513
	L8	186.4993	27	3.62394	29.75	0.121813109
	L31	193.2269	55	7.38210	29.5	0.250240678
Retrograde	L19	202.3801	98	13.15356	29.75	0.442136471
	L30	206.7589	119	15.97218	29.5	0.541429831
	L17	216.0131	173	23.22006	29.75	0.780506218
	L29	232.2419	306	41.07132	29.75	1.380548571
	L28	232.36	271	36.37362	29.75	1.222642689

b